



Preparation and Characterization of Collagen /Alginate Biocomposite Functionalized with Graphene Oxide for Wound Healing Applications

Sivaranjani¹, Pandimadevi M^{1*}

¹Department of Biotechnology, School of Bioengineering, SRM University, Kattankulathur, India

Abstract : The present work aims at fabricating a novel scaffold consisting of Collagen/Alginate/Graphene oxide as a biomaterial to be used in wound healing. Collagen was extracted from Chrome Leather Wastes (CLW) and is used in wound dressings because of its properties like biodegradability, biocompatibility, nontoxicity, ability to absorb large amounts of exudates, etc. Alginate, a naturally occurring biopolymer is used in addition to collagen because of its excellent biocompatible, biodegradable, cell affinity, gelling, non-antigenic, chelating ability, immobilization of specific ligands, physical and chemical cross-linking properties. Graphene oxide, synthesized by modified method is used to prepare the biocomposite for its high mechanical strength. The surface morphology was studied using SEM showed sponge-like appearance indicating the presence of collagen, alginate, and graphene oxide. FTIR and FTRAMAN were employed to characterize the scaffold. TGA proved that the scaffold was stable at high temperature. Other physicochemical characterizations like antibacterial activity and water absorption capacity were carried out to study the effect of graphene oxide in combination with collagen and alginate. Since, collagen and alginate are used as separate biomaterials for wound dressing showed good results, a combination of both incorporated with GO was checked for results and it showed a great improvement in all the properties.

Keywords : Wound healing, collagen, alginate, graphene oxide, biocomposite, TGA.

1.Introduction

Severe wound dehydration would disturb the ideal moist healing environment and delay wound healing. Therefore, substantial efforts are being made to develop new materials for protecting damaged skin from infections and dehydration (Field et al., 1994). The traditional dry dressings such as cotton, wool, natural or synthetic bandages and gauzes are significant for the initial stages of wound healing, but they are dry and cannot provide a moist environment, while they are also often liable to adhere to desiccated wound surfaces and finally induce trauma upon removal (Radhakumary et al., 2011). In order to overcome these drawbacks, researchers, inspired by the concept of moist wound healing; have developed various wet dressings (Winter et al., 1966). The principle of moist wound healing challenges the normal physiological process of wound repair; 'dry healing' seen by the formation of a scab. It is recognised that in moist occlusive / semi-occlusive environments, epithelialisation occurs at twice the rate when compared to a dry one (Winter G., 1962). Moisture under occlusive dressings not only increases the rate of epithelialization, but also promotes healing through moisture itself. Maintaining a moist wound environment facilitates the wound-healing process and moist wound healing is one of the most frequently used, but least understood terms in wound care. Although no reliable

operational definitions exist about the wound surface moisture, a low water vapor transmission rate (WVTR) of a wound dressing has proven to be a reliable measure of a dressing's capacity to retain moisture and provide an environment that supports healing, but at the same time may not be suitable for all types of wounds (Bolton et al., 2000). It was revealed that the initial presence of a low oxygen tension, promoting the inflammatory phase (Jones et al., 2006). Necrotic digits due to ischemia/neuropathy should be kept dry and requires close monitoring regularly and these patients experience problems fighting infection (Winter G, 1962). Making the wound with a moist condition includes prevention of tissue dehydration and cell death, accelerated angiogenesis, increased the breakdown of dead tissue and fibrin, and potentiating the interaction of growth factors with their target cells and heals better than with a dry wound management. When the wounds are covered with occlusive dressing, the pain on the wound seems to be significantly reduced. But, there are reports stating that moisture in wound would rather increase the risk of clinical infection (Bale et al., 1997). Many kinds of dressings such as sponge, gel, occlusive or semi-occlusive dressings have been reported (Jinchen et al., 2013). Skin substitutes can be engineered according to the specific functional objectives with deliberate design and fabrication. Until recently, the design specifications of the skin has relied upon the creation of both artificial epidermal and dermal components, and are combined to produce a replacement skin, which can be grafted in wounded place (Boyce et al., 2002). Till now, the materials used as artificial ECM includes the materials derived from naturally occurring materials and those manufactured synthetically. The natural polymers include polypeptides, hydroxyapatites, hyaluronan, glycosaminoglycans (GAGs), fibronectin, collagen, gelatine, chitosan, fish collagen, fibrin, and alginates. Since these biopolymers have the advantage of possessing low toxicity and a low chronic inflammatory response, and are also beneficial in tissue engineering as scaffolds, hydrogels and films. In the case of synthetic materials, such as polyglycolide, polylactide, polylactide coglycolide, poly vinyl chloride, poly ethylene glycol, poly-tetra-fluoro-ethylene and polyethylene terephthalate are used for sutures and meshes (Vats et al., 2003).

The application of traditional dressing materials and biomaterial-based dressings on the wound area are restricted due to the factors such as their stability problems and risk of infection. Now, the research works are focused on the preparation of wound dressing that are cheaper, effective, and having long shelf-life. Based on the physical, chemical, and biological properties of biopolymers, different types of wound dressings are available in the market. The use of biopolymers as a hemostatic agent depends on its biocompatibility, biodegradability, non immunogenicity, non inflammatory, non allergicity, porosity and optimal mechanical property. Many dressing materials have ideal features for the treatment of wounds and burns; however, due to the variations between pathophysiology of the wound and burn, makes difficult to fabricate and develop an artificial dressing material that are essential for optimum healing mechanisms such as inflammation, tissue replacement, fibrosis, coagulation, etc., (Still et al., 2003).

1.1. Collagen

Collagen is the major protein of the extracellular matrix (ECM) and is the most abundant protein found in mammals, comprising 25% of the total protein and 70% to 80% of skin (dry weight) and is a structural scaffold in tissues. The central feature of all collagen molecules is the stiff and triple-stranded helical structure. Types I, II, and III are the main types of collagen found in connective tissue and constitute 90% of all collagen in the body (Brett, 2008). Type IV, in contrast, forms a two-dimensional reticulum; several other types associate with fibril-type collagens, linking them to each other or to other matrix components. At one time it was thought that all collagens were secreted by fibroblasts in connective tissue, but now, it is known that numerous epithelial cells make certain types of collagens. The various collagens and the structures of them served the same purpose, and help the tissues withstand stretching (Sezer et al., 2011).

Research on wound healing has focussed on the concerned with the events occurring during the first few weeks after wounding. This includes epithelial migration, wound contraction, and gain in tensile strength. In contrast, comparatively little attention has been paid to events in the later stages of healing during which, the young collagen matures and healing of wound continues to become stronger (Douglas et al., 1969). Previously, collagen were thought to function only as structural support; however, collagen and collagen-derived fragments control many cellular functions, including cell shape and differentiation, migration, and synthesis of a number of proteins. Collagen plays an important role in each of these phases of wound healing due to its chemotactic role. It attracts cells such as fibroblasts and keratinocytes to the wound. This encourages debridement, angiogenesis, and re-epithelialisation (Weber et al, 1984; Zbigniew, 2003). Type 1 collagen, specifically, a natural polymer in mammals exhibits favourable characteristics for promoting cell proliferation. It has many

applications in medicine as a matrix to regenerate tissues. It creates a good matrix for the endothelial cell *in vitro*, induce platelet aggregation, promoting blood clotting and consequently accelerate the healing of skin wounds. Although factors such as collagen type, number and nature of molecular cross-links play a role, one of the primary determinants of the mechanical properties of any collagenous tissue is the organization of collagen fibres within the tissue (Whittaker, 1998).

Collagen components such as fibroblast and keratinocytes are fundamental to the process of wound healing and skin formation. Native intact collagen provides a natural scaffold or substrate for new tissue growth (Ruszczak, 2003). Dressings containing collagen are thought to provide the wound with an alternative collagen source that can be degraded by the high levels of MMPs as a sacrificial substrate, leaving the endogenous native collagen to continue normal wound healing (Brett, 2008). There are a number of different collagen dressings available that use a variety of carriers and combining agents such as gels, pastes, polymers and oxidized regenerated cellulose (Brett, 2008).

1.2. Sodium alginate

Alginate is a collective term for a family of polysaccharides produced by brown algae and bacteria (Gorin et al., 1966). This polysaccharide was recognized as a structural component of marine brown algae (Phaeophyceae), where it constitutes up to 40% of the dry matter and occurs mainly in the intercellular mucilage and algal cell wall as an insoluble mixture of calcium, magnesium, potassium, and sodium salts (Haug et al., 1967). Sodium alginates are highly absorbent, gel-forming materials with hemostatic properties. And it has long been known that more rapid healing occurs when a gel is formed at the wound surface and dehydration is prevented. The presence of alginate provides the mechanical strength and flexibility of the seaweed and, additionally, acts as water reservoir preventing dehydration when exposed to air. Alginate can thus be regarded as having the same morpho-physiological properties in brown algae as those of cellulose and pectins in terrestrial plants. Alginates meet all the requirements for their use in pharmaceutical and medical applications. They have been largely used in wound dressings, dental impression, and formulations for preventing gastric reflux. However, the most advanced biotechnological and biomedical application of alginate resides in its use as a hydrogel for cell immobilization for applications ranging from production of ethanol from yeast cells and of antibiotics or steroids (Smidsrød et al., 1990) to transplantation and cell therapy (Lim et al., 1980; Winn et al., 1991; Hasse et al., 2000).

Large quantities of alginate dressings are used each year to treat exuding wounds, such as leg ulcers, pressure sores, and infected surgical wounds. Once in contact with an exuding wound, an ion-exchange reaction takes place between the calcium ions in the dressing and sodium ions in serum or wound fluid. When a significant proportion of the calcium ions on the fibre have been replaced by sodium, the fibre swells and partially dissolves forming a gel-like mass. The degree of swelling is determined principally by the chemical composition of the alginate, which depends on its botanical source. It is also believed that the level of bioactivity of the wound dressings increases due to the presence of an endotoxin in alginates. It also acts as a cross-linker eliminating the use of extraneous cross-linking agents. Due to all these benefits, use of alginates in wound healing is considered an advantageous one (Balakrishnan et al., 2005).

Sodium alginate has been widely adopted as a carrier to immobilize or encapsulate drugs, bioactive molecules, proteins, and cells, for its biocompatible and biodegradable nature. There are many types of alginate-based carriers, such as hydrogels, colloidal particles, and polyelectrolyte complexes, and some of them have been used practically. A number of researchers have studied the combination of alginate-based hydrogels, porous scaffolds and microspheres for controlled drug delivery in tissue engineering (Mi et al, 2003). The physical properties of the alginate hydrogel can be designed to easily match those of articular cartilage in addition to matching the mechanical properties of the scaffold with the native tissue. Alginate-based injectable hydrogels, solid- and gel-microspheres have been used in cartilage regeneration. (Cooper et al.,2010).

1.3 Graphene Oxide

Graphene oxide (GO) is a highly oxidized form of chemically modified graphene that consists of a single-atom-thick layer of graphene sheets with the carboxylic acid, epoxide and hydroxyl groups in the plane, and are microns or larger in size. The peripheral carboxylate group provides colloidal stability and pH dependent negative surface charge (Park et al., 2009). Epoxide (-O-) and hydroxyl (-OH) groups present on the

basal plane are uncharged but polar, allowing weak interactions, hydrogen bonding and other surface reactions (Kim et al., 2013).

Although the exact structure of GO is difficult to determine, it is clear that for GO the previously contiguous aromatic lattice of graphene is interrupted by epoxides, alcohols, ketone carbonyls, and carboxylic groups (Marcono et al., 2010). The intensive research on the bio-applications of graphene and its derivatives is due to many fascinating properties, such as high specific surface area (2630 m²/g), exceptional electronic conductivity (mobility of charge carriers, 200,000 cm²V⁻¹ s⁻¹), thermal conductivity (~5000 W/m/K), mechanical strength (Young's modulus, ~1100 Gpa) of graphene, and, intrinsic biocompatibility, low cost and scalable production, and facile biological/chemical functions of GO (Sheng et al., 2012).

First, rational functionalization chemistry is needed to impart graphene with aqueous solubility and biocompatibility. GO and its chemically converted derivatives form stable suspensions in pure water but generally aggregate in salt or other biological solutions. Second, graphene sheets with suitable sizes are desired. Size control or size separation on various length scales is necessary to suitably interface with biological systems *in vitro* or *in vivo*. Lastly, little is known experimentally about the properties of graphene with molecular dimensions, on the order of ~10 nm or below. The optical properties of graphene and GO, a topic of fundamental interest, are largely unexplored and could facilitate biological and medical research such as imaging (Sun et al., 2008).

Graphene nanosheets identically show some similar properties to carbon nanotubes (CNTs), but in the case of cytotoxicity studies, single-wall and multiwall CNTs show more toxicity to human and animal cells compared to graphene derivatives. This is due to the fact that GO is a two-dimensional structure, whereas CNTs have only a single dimension. GO in addition to antimicrobial properties encourages the proliferation of cells on its surface. The material was, in fact, toxic to some micro-organisms while being safe for human. Hence, GO in combination with other nanoparticles like AgNPs showed efficient antibacterial activity against both gram negative and gram positive organisms. Due to concentration dependent toxicity, GO cannot be directly used in cell culture applications, however, GO can be functionalized with biomacromolecules for biomedical application (Sastry et al., 2014). Graphene oxide (GO) as an efficient nanocarrier for drug delivery (Liu et al., 2008). GO, is an ideal nanocarrier for efficient drug and gene delivery. GO used for drug delivery is usually 1-3 layers (1-2 nm thick), with size ranging from a few nanometers to several hundred nanometers. The unique structural features, such as large and planar sp² hybridized carbon domain, high specific surface area (2630 m²/g), and enriched oxygen-containing groups, render GO excellent biocompatibility, and physiological solubility and stability, and capability of loading of drugs or genes via chemical conjugation or physisorption approaches (Sun et al., 2008).

In the present work, collagen was extracted from chrome containing leather waste which is a major by-product of leather industry. Graphene oxide was synthesized using modified Hummer's method to be incorporated with the extracted collagen. A film was prepared using collagen, graphene oxide and sodium alginate after the optimization of their concentration and physicochemical properties were analyzed. Finally, a film containing collagen, alginate and graphene oxide was prepared, along with gauze and characterized. The antibacterial studies were done on the prepared film. These biopolymers are beneficial in tissue engineering as scaffolds, hydrogels, and films.

2. Materials and Methods

2.1. Materials

5% sodium hydroxide, Conc. sulphuric acid, 30% Hydrogen peroxide, sodium alginate, ethylene glycol, graphite, potassium permanganate, 5% hydrochloric acid, acetone and distilled water. All the reagents are of analytical grade.

2.2. Extraction of collagen

Chrome containing Leather Wastes (CCLW) was soaked in 5% sodium hydroxide solution for 24 hours. It was then washed with tap water until pH 7. Treatment of the obtained sample with 10-15 mL of conc. sulphuric acid dechromes the collagen. Repeated washing was carried out to bring the pH back to basic. This

step was repeated continuously until pH7 is reached. Hydrogen peroxide is used as a bleaching agent and the final collagen is obtained as a paste. The obtained collagen was refrigerated at 4°C.

2.3. Optimization of collage & alginate for film formation

The concentration of collagen and alginate were varied to optimize the stoichiometric ratios. For the concentration optimization, 1 to 5g of collagen was taken and added with 1 to 5g of alginate. Finally a ratio of C: A (2.5:1) was obtained for a perfect film.

Table 1. Optimization of Collagen and Alginate concentration

Sample No.	Ratio of Collagen/Alginate (g/g)				
	1:1	1:2	1:3	1:4	1:5
1.	1:1	1:2	1:3	1:4	1:5
2.	1.5:1	1.5:2	1.5:3	1.5:4	1.5:5
3.	2:1	2:2	2:3	2:4	2:5
4.	2.5:1	2.5:2	2.5:3	2.5:4	2.5:5
5.	3:1	3:2	3:3	3:4	3:5
6.	3.5:1	3.5:2	3.5:3	3.5:4	3.5:5
7.	4:1	4:2	4:3	4:4	4:5
8.	4.5:1	4.5:2	4.5:3	4.5:4	4.5:5
9.	5:1	5:2	5:3	5:4	5:5

2.4. Preparation of Collagen/Alginate film

Collagen-Alginate films were prepared by varying different stoichiometric ratios of collagen and alginate are given in Table 1. 25 grams of collagen was taken and mixed well with 10 grams of alginate. This was further diluted by adding 200mL of distilled water and further mixed using a stirrer. The addition of 2mL of Ethylene glycol would increase the flexibility of the final film. After stirring for few minutes, the mixture was poured into polythene trays (measurement 12 cm x 7.5 cm) and dried at room temperature (30°C) to get C/Al/GO in sheet form.

2.5. Preparation of GO using modified Hummers method (2010)

Graphene oxide was prepared using Modified Hummers method (2010). 1g of graphite and 1g of sodium nitrate was added to 23 mL of Conc. sulphuric acid at 0°C and stirred for 4 hours. 6 grams of potassium permanganate was added to the above solution with continuous stirring for 2 hrs. 92 mL of distilled water was added slowly and the temperature was raised to 90°C for 15 mins. 200 mL of distilled water and 20 mL of 30% H₂O₂ were added subsequently and left overnight undisturbed. The solution was centrifuged at 6000 rpm and washed with water and 5% HCl alternatively till the pH reached 7. The final residue was dried at 60°C in hot air oven.

2.6. Preparation of collagen/alginate & graphene oxide incorporated bandage gauze

Depending upon the characterization results obtained for the Collagen/ Alginate film, the best ratio of (2.5:1) was chosen and it was optimized with different ratio of GO.

Table 2: Optimization of Collagen/Alginate/GO for the preparation of bandage gauze

Sample No.	Collagen(g)	Alginate (g)	Graphene Oxide(g)
1	2.5	1	0.1
2	2.5	1	0.3
3	2.5	1	0.5
4	2.5	1	0.7
5	2.5	1	1

The prepared films of different ratios of Collagen/ Alginate/ GO are shown in Table 2. The films were analyzed using different characterization tests like tensile strength, biodegradability, and antibacterial activities before and after the inclusion of bandage gauze.

3. Characterization

3.1 Tensile strength

Tensile strength properties were measured using three dumb-bell shaped specimens of 4 mm wide and 10 mm length of prepared films. Mechanical properties such as tensile strength (Mpa) and percentage of elongation at break (%) were measured using a Universal testing machine (INSTRON model 1405) at an extension rate of 5 mm/min.

3.2 Thermogravimetric analysis

Thermogravimetric analysis was carried out using Universal V4.4A TA Instrument. It is a technique in which the mass of a substance is monitored as a function of temperature or time as the sample specimen is subjected to a controlled temperature program in a controlled atmosphere.

3.3 FTIR

Fourier transform infrared (FTIR) measurements were carried out to determine the formation and changes in the functional groups on the prepared composite films. The spectra were measured at a resolution of 4 cm⁻¹ in the frequency range of 4000–500 cm⁻¹ using Nicolet360 FTIR spectrometer.

3.4 FT-Raman

The FT-Raman spectrum was carried out using Bruker RFS 27 FT-Raman spectrometer, with a scanning range of 50-4000cm⁻¹.

3.5 Scanning electron microscope

Surface morphology of the samples was visualized by scanning electron microscope (SEM Model LEICA stereo scan 440). The samples were coated with gold ions using an ion coater (Fisons sputter coater) with following parameters: 1 Torr pressure, 20 mA current, and 70 coating time, using a 15 kV as accelerating voltage. Atomic force microscopy (AFM) was done with Agilent Pico LE Scanning Probe Microscope model. The Agilent instrument is a tip scan instrument, equipped with small (10 ml) and large AFM scanners (150 ml). This instrument is equipped with an environmental chamber, capable of heating to 200°C.

3.6 Biodegradability

The water absorption capacities of C/ Al and C/ Al/ GO biocomposite were determined according to the method followed by Sastry et al., 2014. To measure the biodegradability of the sample, the weight of the scaffold was measured as a function of degradation time. Three specimens of all scaffolds were equally weighed (W_0) and then immersed in water for 24 h. The temperature was maintained at 37°C. After predetermined periods of soaking time (1 hour), each specimen was taken out and, the superficial water was blotted on filter paper and the scaffolds were then weighed (W_T). The percentage of weight loss was calculated using the following equation,

$$\text{Weight loss (\%)} = ((W_0 - W_T) / W_0) * 100.$$

3.7 Antibacterial activity

Two bacterial cultures were chosen for antimicrobial activity namely *Staphylococcus aureus* (NCIM 5021) and *E.coli* (NCIM 293). All the cultures were subcultured periodically and maintained on nutrient agar at room temperature. The activity was found by disc diffusion method. Muller Hinton agar was sterilized and poured onto petriplates and allowed to solidify under laminar air flow. About 100 microliters of the bacterial samples each was streaked on separate plates. Antibacterial sensitivity was carried out by cutting the produced

scaffolds as discs and using them as samples. They were impregnated into the cultured bacterial plate and left undisturbed for 24 hours. This test is performed against both grams positive and gram negative bacteria.

4.0 Results and Discussion

4.1 FT-Raman

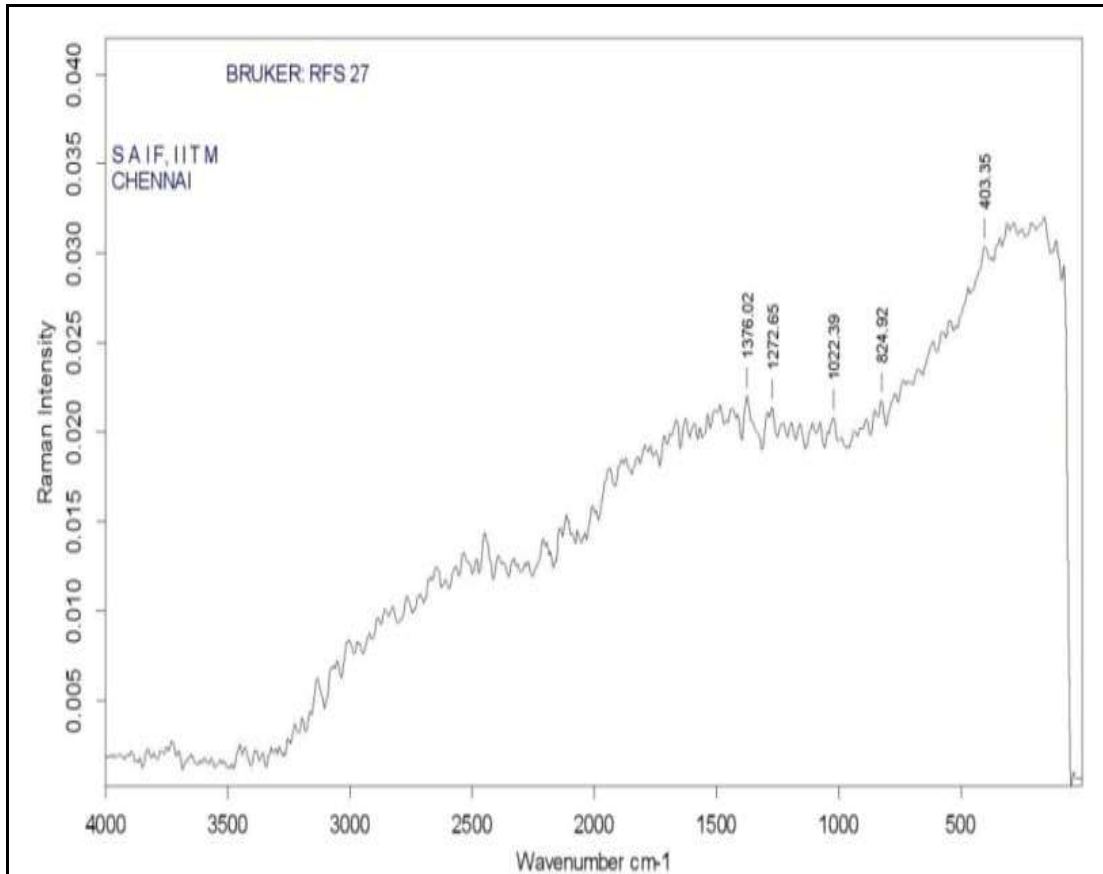


Fig.1: FT-RAMAN of prepared graphene oxide

FT-RAMAN spectrum of graphene oxide are given in figure 1. It was observed that there are 2 peaks at 1376.02 cm^{-1} (G band), and 1272.65 cm^{-1} (D band). The G peak corresponds to the optical E_{2g} mode of graphite related to the bond vibration of sp^2 bonded carbon atoms in a 2-dimensional hexagon lattice. The D peak is an indication of disorder in the Raman of the GO, originating from the defects associated with grain boundaries, vacancies and amorphous carbon species in the sample. The intensity ratio of D to G band is generally accepted, reflecting the graphitization degree of carbonaceous materials and defect density. I_D/I_G of pristine GO is 0.98.

4.2 FTIR

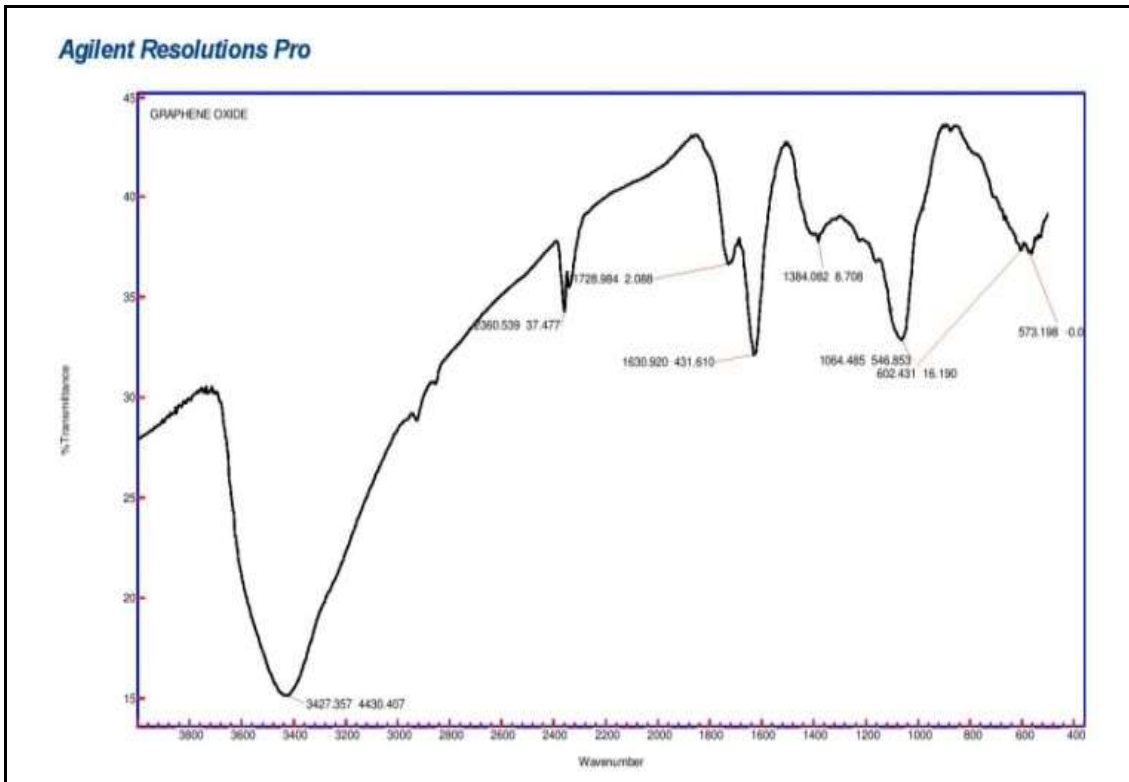


Fig. 2. FTIR of prepared graphene oxide

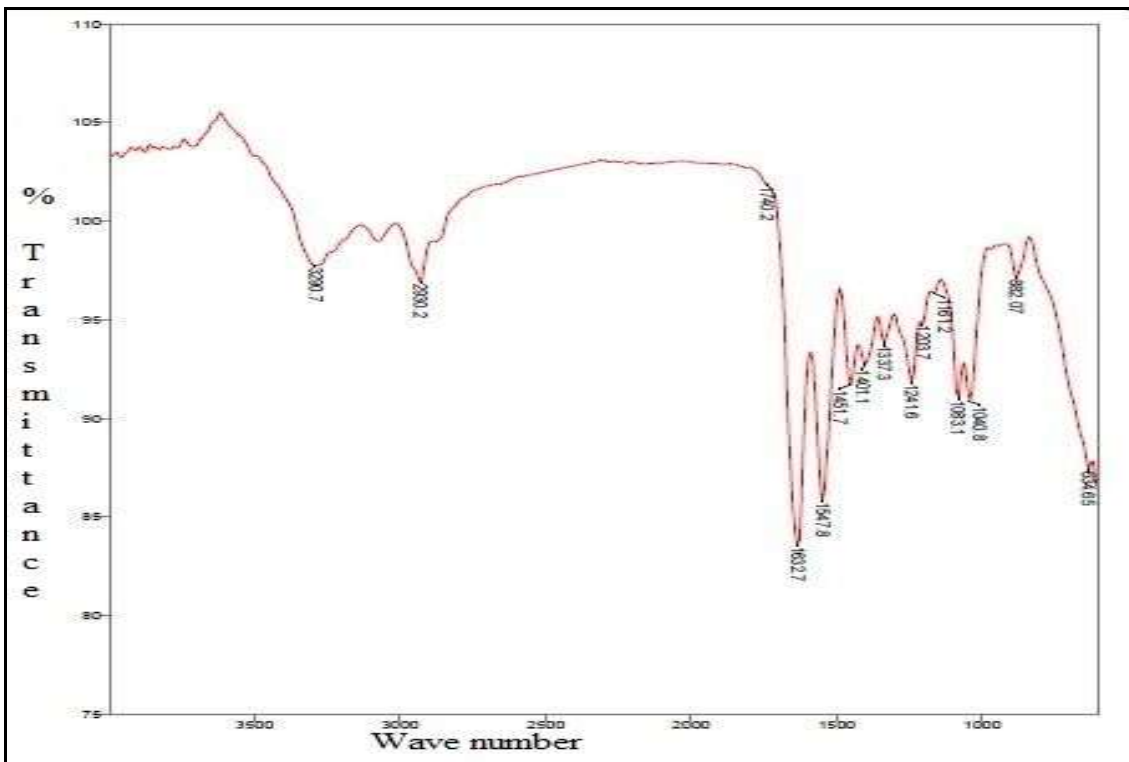


Fig 3: FTIR of collagen/alginate/GO

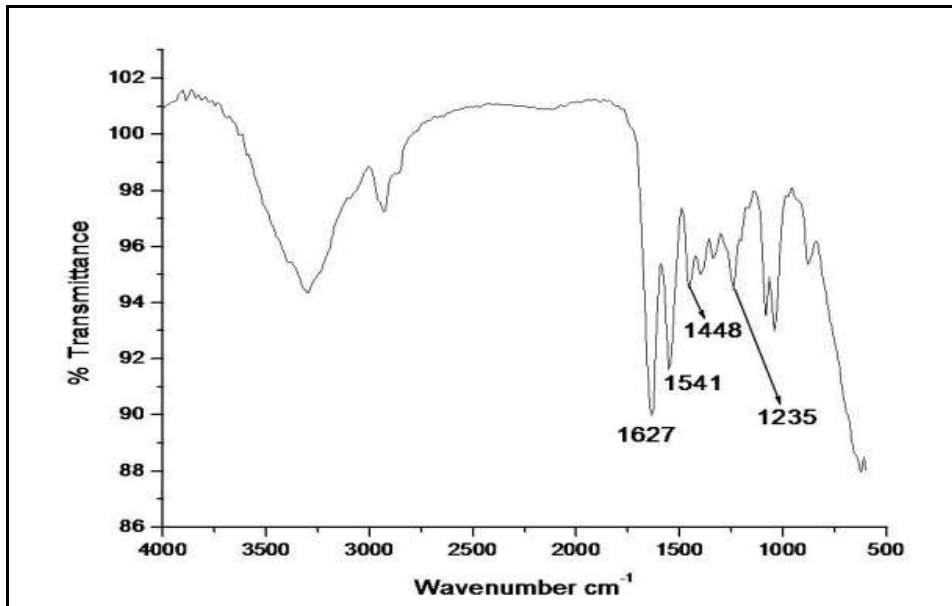


Fig .4 . FTIR of extracted collagen

The FT-IR spectrum of GO are given in Fig.2 The presence of different types of oxygen functionalities in GO was confirmed at broad and wide peak at 3447 cm^{-1} and 2360 cm^{-1} can be attributed to the O-H stretching vibrations of the C-OH groups and water. A peak at 1728 cm^{-1} is due to the carboxy groups present in the sample. The absorption bands at 1627 cm^{-1} can be ascribed to benzene rings. The sharp intense peak at 1448 cm^{-1} can be attributed to CO carboxylic. The peak at 1235 cm^{-1} and 1064 cm^{-1} confirms the presence of epoxy and alkoxy groups respectively. The FT-IR spectrum of Collagen/ Alginate/ GO are shown in Fig.3. The loss of peak at 1740.2 cm^{-1} confirms that GO is functionalized. The FT-IR of collagen is shown in Fig.4. Since collagen is a protein, they have exhibited characteristic absorption bands. The peaks at 1632.7 cm^{-1} , 1547.8 cm^{-1} , and 1203.7 cm^{-1} represent amide peaks of collagen. Comparing the results of (Sastry et al., 2014) the absorption intensities between amide 3 and amide 2 groups are nearly equal to 1.0 which confirms the triple helical structure of collagen. The carboxyl peaks of alginate and GO are found at 1416 cm^{-1} and 1357 cm^{-1} respectively. The peak at 1241.68 cm^{-1} is due to the carbohydrate groups present in collagen.

4.3 Thermo gravimetric analysis

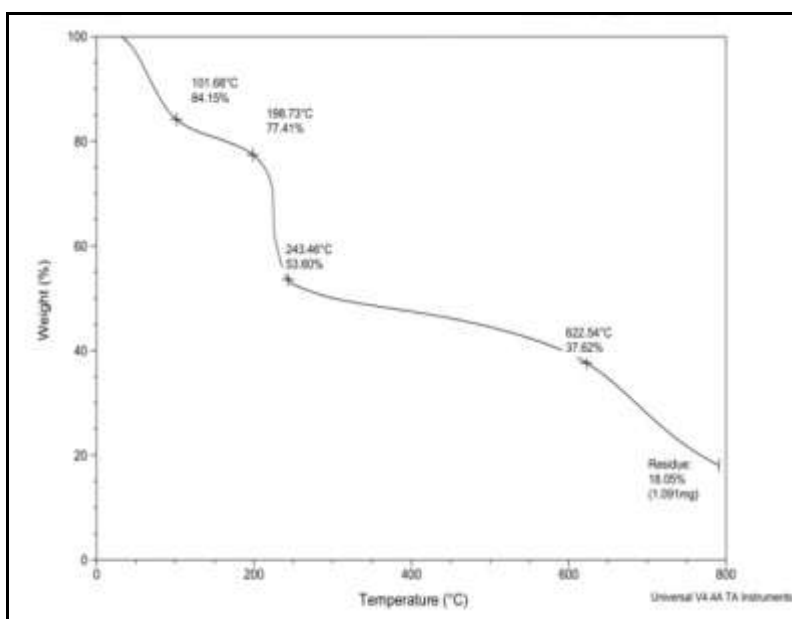


Fig. 5. TGA of prepared GO

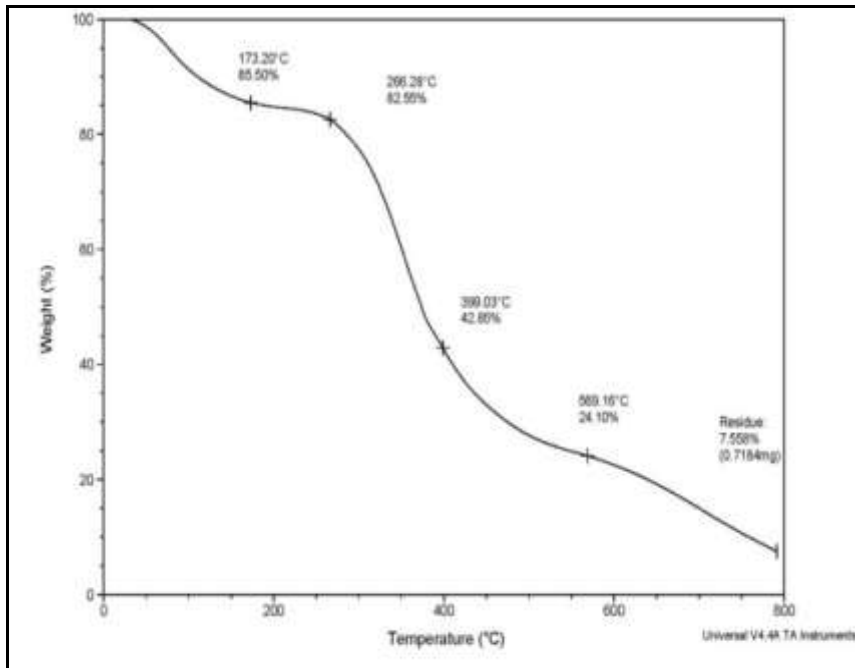


Fig 6. TGA of Collagen/Alginate

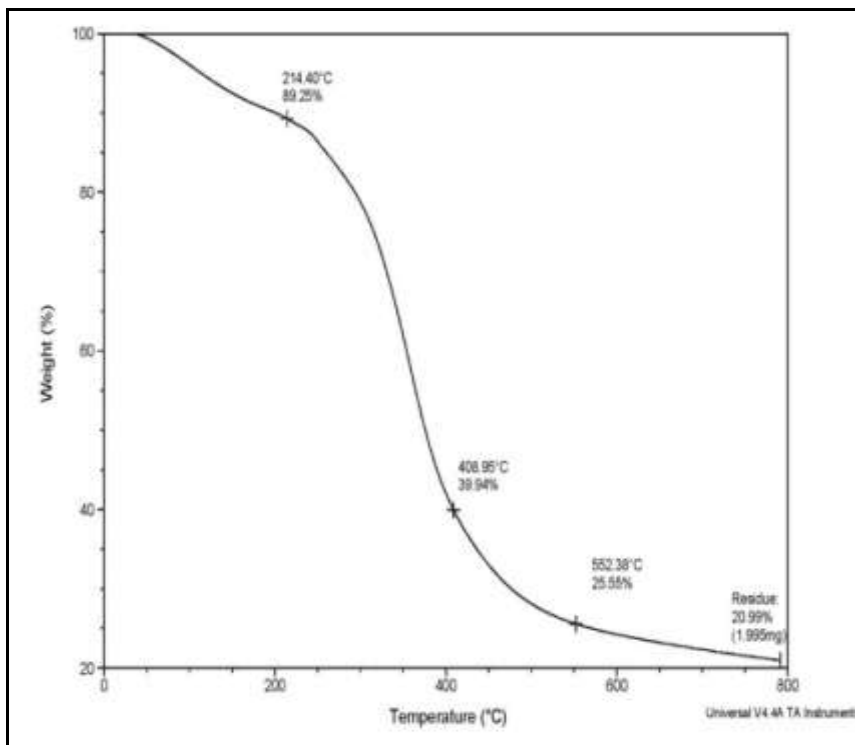


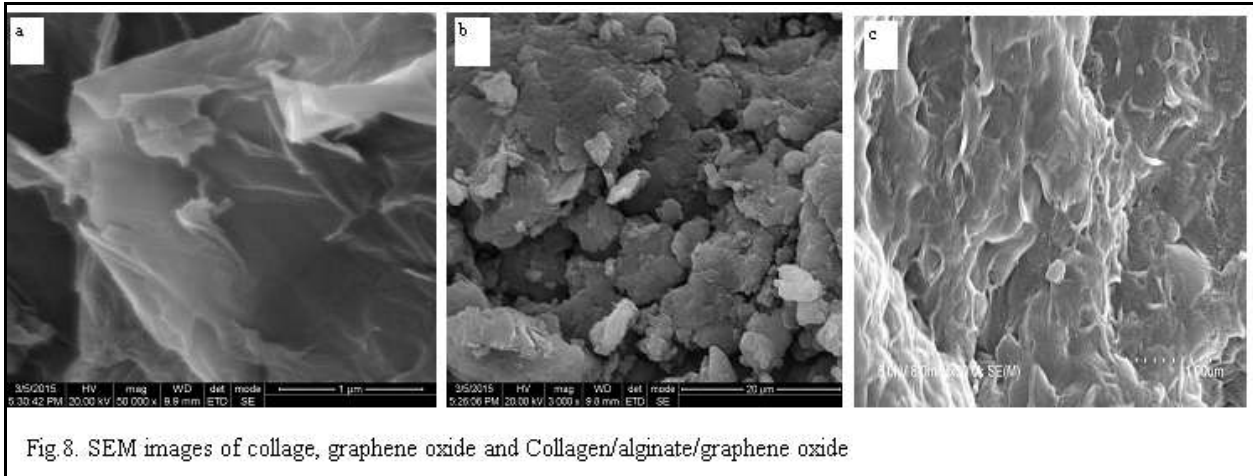
Fig 7. TGA of Collagen/Alginate/GO

FT-IR spectrum of fibrin, chitosan and sodium alginate and F-C-SA are given in figure 1.

The TGA of GO was shown in Fig.5 and it shows that GO was highly stable up to 800 °C. GO shows slight mass decrease from room temperature to 150° C and significant decrease from 150° C to 200° C. The first 15.85% (~102° C) mass loss was due to water solvent molecules absorbed into the GO bulk material, the following 22.59% (~199° C) stands for the elimination of remaining functional groups. The major mass loss at 200° C was due to the pyrolysis of liable oxygen-containing functional groups, generating CO, CO₂, and steam. Further decomposition takes place at 800° C. Even at 800° C, 0.05% of GO was left.

The TGA curve of Collagen/ Alginate composite was shown in Fig.6. The resultant composite was stable up to 800° C. It is seen that maximum mass loss occurs at 400° C. It occurs in 4 steps such as the first loss at ~225°C is due to dehydration, the second loss at 400° C is due to depolymerization and the third loss at (approx 575° C) can be attributed to the evolution of gases. The final residue left is 7.558% at 800° C. The TGA curve of collagen/alginate/GO was shown in Fig.7, it was observed that the maximum mass loss occurs at (~40%) 400° C. This might be due to the dehydration and the next loss was due to the evolution of gases. However, it was observed that ~21% of the residue was left at 800°C which was higher than the Collagen/ Alginate composite. Thus, it proves that the final scaffold is more stable at 800° C.

4.4 Scanning Electron Microscope



SEM pictures of the prepared collagen, GO and collagen/sodium alginate/GO is shown in Fig.8. It also shows that GO particles have a layered structure. GO shows agglomeration of ultrathin sheets; the surface of Collagen/ Alginate was smooth and porous in nature. It appears sponge-like which is due to the presence of collagen. The presence of GO was evident in Collagen/ Alginate/ GO and it had retained its porosity even after the addition of GO. The porous nature of the Collagen/Alginate/GO film helps in absorbing the wound exudates and also helps in oxygen exchange to the wound surface.

4.5 Tensile strength

Table 3: Tensile strength of Collagen and Alginate scaffolds

Sample No.	Ratio	Elongation at break (%)	Tensile strength (MPa)
1.	C:A (2.5:0.5)	36.28± 0.24	19.83± 0.21
2.	C:A (2.5:1.0)	45.55± 0.15	21.92± 0.43
3.	C:A (2.5:1.5)	28.25± 0.09	13.42± 0.22
4.	C:A (2:0.5)	19.25± 0.31	6.75± 0.31
5.	C:A (2:1)	23.65± 0.42	20.42± 0.14
6.	C:A (2:1.5)	22.98± 0.11	8.33±0.31
7.	C:A (1.5:0.5)	14.31± 0.23	6.08± 0.47
8.	C:A (1.5:1.0)	39.98± 0.31	11.58± 0.14
9.	C:A (1:1)	38.05± 0.05	21.17± 0.23
10.	A:C (2:0.5)	29.50± 0.33	17.67± 0.56
11.	A:C (2:1)	36.16± 0.26	18.33± 0.38
12.	A:C (2:1.5)	28.26± 0.27	10.25± 0.19

Table 4: Tensile strength of Collagen/Alginate/GO

Sample No.	C:Al:GO	% Elongation at break	Tensile strength (MPa)
1.	2.5:1:0.1	37.80± 0.47	26.83± 0.54
2.	2.5:1:0.3	45.77 ±0.67	28.50 ± 0.14
3.	2.5:1:0.5	27.05± 0.74	24.00± 0.28
4.	2.5:1:0.7	20.89± 0.36	28.50± 0.32
5.	2.5:1:1	13.08± 0.27	8.17± 0.42
6.	2.5:1:0.3(Cotton Gauze)	65.52 ± 0.84	40.83 ± 0.38

The tensile strength of collagen and alginate films are shown in the Table 3. And the tensile strength of collagen, alginate and GO films are shown in the table 4. The mechanical properties of wound dressing material play a major role. The tensile strength and the elongation at break properties were studied on the prepared film. In the case of collagen/ Alginate films, it was found that with increasing concentrations of alginate the tensile strength decreased. In the case where least concentration of collagen was used, the film had the least tensile strength. This proves that collagen increases the tensile strength. Among the different stoichiometric ratios used, the C: Al (2.5:1) had better tensile strength when compared to others. Hence, GO was incorporated into a fore mentioned ratio and its tensile strength was analyzed. In this case, it was seen that as the concentration of GO increased the tensile strength also increases but starts lowering after a particular value. The ratio of C: Al: GO (2.5:1:0.3) proved to have the best tensile strength. When gauze was incorporated to the above-mentioned ratio, its tensile strength increased to almost double.

4.6 Water absorption ability

Hydrolysis is the main factor that determines the water uptake ability of the sample. It plays a major role in the absorption of exudates which will keep the wound surface dry and prevent further infection thereby enhancing healing. The water absorption capacities of the prepared films were done to check for above-mentioned properties and the values are as mentioned in the Fig. 9. Here, the table shows that the ratio of C: A: GO (2.5:1.0:0.3) has the highest water absorption ability within 2 hours.

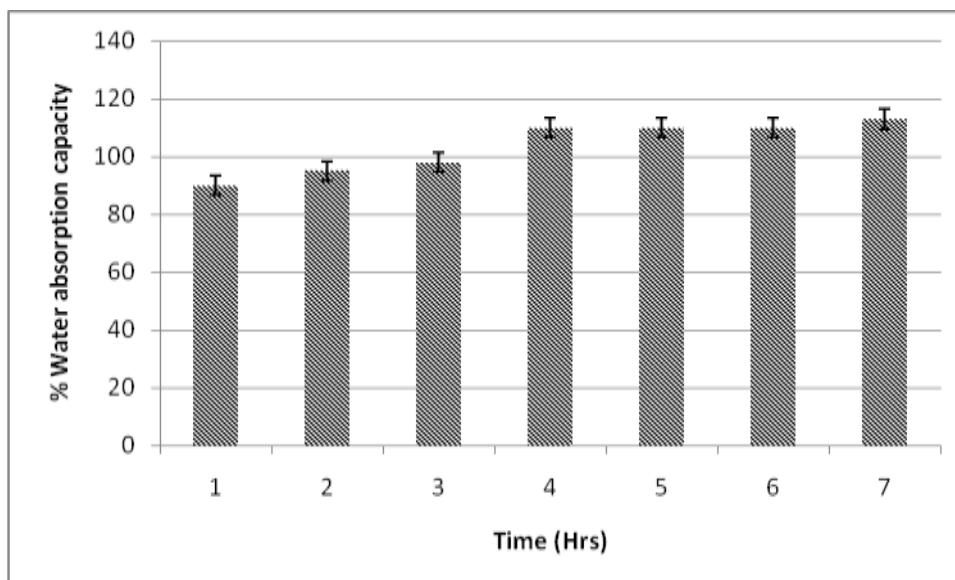


Fig 9. Water absorption ability of Co:Al:GO in the ratio of 2.5:1:0.3 The data are represented as the mean± standard deviation; n = 3

4.7 Antibacterial activity of *E.coli* and *S.aureus*

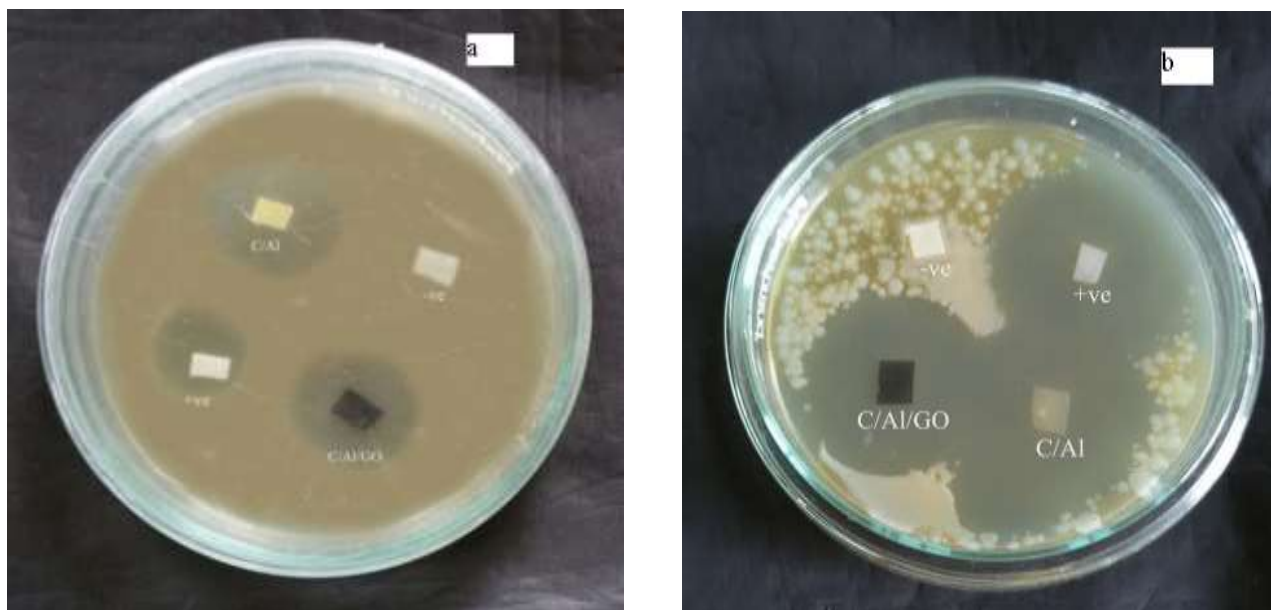


Fig.10 (a) Zone of inhibition of *E.coli*

(b) Zone of inhibition of *S.aureus*

The antibacterial activities are shown in the Fig. 10 (a) and (b). Antibacterial activity was tested with the scaffolds against a gram positive and gram negative bacteria. This was to check if the film had properties to prevent the bacterial growth on the surface of the wounds. The property was identified by the zone of inhibition. The scaffolds were impregnated on culture plates containing Gram positive (*S.aureus*) and Gram negative (*E.coli*). The result showed that the resultant film had antibacterial activity against both types of bacteria. Streptomycin was used as a positive control and a filter paper dipped in gauze as negative. Clear zones were seen around the films. The zone of clearances were bigger than the positive control in gram-positive bacteria whereas the zones have unified in the gram-negative plate.

5.0 Summary and Conclusion

A composite film containing Collagen/ Alginate/ Graphene oxide was synthesized and tested for their application in wound healing. Collagen was synthesized from leather industry wastes which are a cheap source. Graphene oxide was prepared using modified Hummer's method. Then this Collagen (C) and Graphene oxide (GO) was used along with alginate (Al) to synthesis a novel C/ Al/ GO biocomposite. FT-IR analysis suggested the presence of all the components in the composite and the Graphene oxide was found to be functionalized in the composite. The addition of alginate improved the gel forming properties of the final film. Incorporation of GO increased the mechanical strength of the resultant film. Among different stoichiometric ratios of C/ Al/ GO composites prepared, composite with C/ Al/ GO in the ratio 2.5:0.3:0.3 (w/v) was found to possess better mechanical, biodegradable properties and antimicrobial properties. Therefore from the results obtained, the final composite could be suggested to have a potential application as a wound dressing material.

References

1. Akhavan, O., Ghaderi, E., Toxicity of graphene and graphene oxide nanowalls against bacteria. *ACS nano*, 2010, 4(10), 5731-5736.
2. Balakrishnan, B., Mohanty, M., Umashankar, P. R., Jayakrishnan, A. Evaluation of an in situ forming hydrogel wound dressing based on oxidized alginate and gelatin, *Biomaterials*, 2005, 26(32), 6335-6342.
3. Boyce, S. T., & Warden, G. D., Principles and practices for treatment of cutaneous wounds with cultured skin substitutes, *The American journal of surgery*, 2002, 183(4), 445-456.
4. Cao, Y., Shen, X., Chen, Y., Guo, J., Chen, Q., & Jiang, X., pH-induced self-assembly and capsules of sodium alginate. *Biomacromolecules*, 2005, 6(4), 2189-2196.

5. Field, C. K., & Kerstein, M. D., Overview of wound healing in a moist environment, *The American journal of surgery*, 1994, 167(1), S2-S6.
6. Cooper, C., Snow, S., McAlindon, T. E., Kellingray, S., Stuart, B., Coggon, D., Dieppe, P. A., Risk factors for the incidence and progression of radiographic knee osteoarthritis. *Arthritis & rheumatism*, 2000, 43(5), 995-1000.
7. Marcano, D. C., Kosynkin, D. V., Berlin, J. M., Sinitiskii, A., Sun, Z., Slesarev, A., Tour, J. M. Improved synthesis of graphene oxide. *ACS nano*, 2010, 4(8), 4806-4814.
8. Deepachitra, R., Ramnath, V., Sastry, T. P., Graphene oxide incorporated collagen–fibrin biofilm as a wound dressing material. *RSC Advances*, 2014, 4(107), 62717-62727.
9. Douglas, D. M., Forrester, J. C., Ogilvie, R. R. Physical characteristics of collagen in the later stages of wound healing. *British Journal of Surgery*, 1969, 56(3), 219-222.
10. Enoch, S., & Harding, K. Review wound bed preparation: the science behind the removal of barriers to healing. *Wounds*, 2003, 15(7), 213-229.
11. Ferretti, M., Marra, K. G., Kobayashi, K., Defail, A. J., Chu, C. R., Controlled *in vivo* degradation of genipin crosslinked polyethylene glycol hydrogels within osteochondral defects. *Tissue Engineering*, 2006, 12(9), 2657-2663.
12. Cioca, G. (1983). U.S. Patent No. 4,412,947. Washington, DC: U.S. Patent and Trademark Office.
13. Gillitzer, R., & Goebeler, M., Chemokines in cutaneous wound healing. *Journal of leukocyte biology*, 2001, 69(4), 513-521.
14. Gorin, P. A. J., & Spencer, J. F. T., Exocellular alginic acid from *azotobacter vinelandii*. *Canadian journal of chemistry*, 1996, 44(9), 993-998.
15. Hasse, C., Bohrer, T., Barth, P., Stinner, B., Cohen, R., Cramer, H., Rothmund, M., Parathyroid xenotransplantation without immunosuppression in experimental hypoparathyroidism: long-term *in vivo* function following microencapsulation with a clinically suitable alginate, *World journal of surgery*, 2000, 24(11), 1361-1366.
16. Chvapil, M. (1974). U.S. Patent No. 3,823,212. Washington, DC: U.S. Patent and Trademark Office
17. Haug, A., & Smidsrød, O. Strontium–Calcium Selectivity Of Alginates. *Nature*. 1967, 215, 757-762.
18. . Hu, W., Peng, C., Luo, W., Lv, M., Li, X., Li, D., & Fan, C., Graphene-Based Antibacterial Paper, *ACS Nano*, 2010, 4(7), 4317-4323.
19. Brett, D. A review of collagen and collagen-based wound dressings. *wounds-A compendium of clinical research and practice*, 2008, 20(12), 347-356.
20. Fan, Z., Liu, B., Wang, J., Zhang, S., Lin, Q., Gong, P. & Yang, S., A novel wound dressing based on ag/graphene polymer hydrogel: effectively kill bacteria and accelerate wound healing. *Advanced Functional Materials*, 2014, 24(25), 3933-3943.
21. William, S., Hummers, J. R., Offeman, R. E., Preparation Of Graphitic Oxide, *J Am Chem Soc*, 1958, 80(6), 1339.
22. Tang, J., Chen, Q., Xu, L., Zhang, S., Feng, L., Cheng, L., Peng, R., Graphene oxide–silver nanocomposite as a highly effective antibacterial agent with species-specific mechanisms, *ACS applied materials & interfaces*, 2013, 5(9), 3867-3874.
23. Sun, J., Tan, H., Alginate-Based Biomaterials For Regenerative Medicine Applications. *Materials*, 2013, 6(4), 1285-1309.
24. Khaled, M.A., Jalila, A., Kalthum, H., Noordin, M., Asma Saleh W (2014). Collagen-Calcium Alginate Film Dressing With Therapeutic Ultrasound To Treat Wounds In Rats, *Research journal of Biological Sciences*, 2014, 9 (2); pp 57-61.
25. Kim, H., & Kim, W. J. (2014). Photo thermally controlled gene delivery by reduced graphene oxide–polyethylenimine nanocomposite, *Small*, 2014,10(1), 117-126.
26. Lee, B. H., Li, B., & Guelcher, S. A. Gel Microstructure Regulates Proliferation And Differentiation Of Mc3t3-E1 Cells Encapsulated In Alginate Beads. *Acta biomaterialia*, 2015, 8(5), 1693-1702.
27. Lim, F., & Sun, A. M., Microencapsulated islets as bioartificial endocrine pancreas, *Science*, 1980, 10(4472), 908-910.
28. Liu, Z., Yang, K., Wan, J., Zhang, S., Tian, B., Zhang, Y. The Influence Of Surface Chemistry And Size Of Nanoscale Graphene Oxide On Photothermal Therapy Of Cancer Using Ultra-Low Laser Power. *Biomaterials*, 2012, 33(7), 2206-2214.
29. Bolton, L. L., Monte, K., Pirone, L. A. Moisture And Healing: Beyond The Jargon. *Ostomy/wound management*, 2000, 46(1A Suppl), 51-62.

30. Sun, J., & Tan, H., Alginate-based biomaterials for regenerative medicine applications. *Materials*, 2013, 6(4), 1285-1309.
31. Donati, I., Paoletti, S., Material properties of alginates. in alginates: biology and applications . Springer Berlin Heidelberg. 2009, 1-53.
32. Radhakumary, C., Antonty, M., Sreenivasan, K., Drug loaded thermoresponsive and cytocompatible chitosan based hydrogel as a potential wound dressing. *Carbohydrate Polymers*, 2011, 83(2), 705-713.
33. Nigam, A. (1990). U.S. Patent No. 4,948,540. Washington, DC: U.S. Patent and Trademark Office
34. Rokstad, A. M., Holtan, S., Strand, B., Steinkjer, B., Ryan, L., Kulseng, B., & Espevik, T., Microencapsulation of cells producing therapeutic proteins: optimizing cell growth and secretion. *Cell transplantation*, 2002, 11(4), 313-324.
35. Donati, I., Paoletti, S., Material properties of alginates. In alginates: biology and applications, Springer Berlin Heidelberg. 2009, 1-53.
36. Sezer, A. D., & Cevher, E. (2011). Biopolymers As Wound Healing Materials: Challenges And New Strategies. *Intech Open Access Publisher*.
37. Shastri, V. P Forget, A., Christensen, J., Lüdeke, S., Kohler, E., Tobias, S., Matloubi, M., Polysaccharide Hydrogels With Tunable Stiffness And Provasculogenic Properties Via A-Helix To B-Sheet Switch In Secondary Structure. *Proceedings of the National Academy of Sciences*, 2013, 110(32), 12887-12892.
38. von der Mark, K., Park, J., Bauer, S., & Schmuki, P., Nanoscale Engineering Of Biomimetic Surfaces: Cues From The Extracellular Matrix. *Cell and tissue research*, 2010, 339(1), 131-153.
39. Goenka, S., Sant, V., & Sant, S., Graphene-Based Nanomaterials For Drug Delivery And Tissue Engineering. *Journal of Controlled Release*, 2014, 173, 75-88.
40. Liu, J., Cui, L., & Losic, D., Graphene and graphene oxide as new nanocarriers for drug delivery applications. *Acta biomaterialia*, 2013, 9(12), 9243-9257.
41. Sun, X., Liu, Z., Welsher, K., Robinson, J. T., Goodwin, A., Zaric, S., & Dai, H., Nano-Graphene Oxide For Cellular Imaging And Drug Delivery, 2008, *Nano research*, 1(3), 203-212.
42. Tan, H., Shen, Q., Jia, X., Yuan, Z., & Xiong, D., Injectable Nanohybrid Scaffold For Biopharmaceuticals Delivery And Soft Tissue Engineering. *Macromolecular Rapid Communications*, 2012, 33(23), 2015-2022.
43. Tanihara, M., Suzuki, Y., Nishimura, Y., Suzuki, K., & Kakimaru, Y., Thrombin-Sensitive Peptide Linkers for Biological Signal-Responsive Drug Release Systems. *Peptides*, 1998, 19(3), 421-425.
44. Vanessa Jones, Joseph E Grey, Keith G Harding, ABC of wound healing. *Wound dressings*, 2006, 332, 122-130
45. Vats, A., Tolley, N. S., Polak, J. M., & Gough, J. E., Scaffolds and biomaterials for tissue engineering: a review of clinical applications, *Clinical Otolaryngology & Allied Sciences*, 2003, 28(3), 165-172.
46. Weber, L., Kirsch, E., Müller, P., & Krieg, T., Collagen type distribution and macromolecular organization of connective tissue in different layers of human skin, *Journal of investigative dermatology*, 1984, 82(2), 156-160.
47. Whittaker, P., Collagen organization in wound healing after myocardial injury. *Basic research in cardiology*, 1998, 93(3), 023-025.
48. Winn, S. R., Tresco, P. A., Zielinski, B., Greene, L. A., Jaeger, C. B., & Aebischer, P. Behavioral Recovery Following Intrastratial Implantation of Microencapsulated PC12 Cells. *Experimental neurology*, 1991, 113(3), 322-329.
49. Winter, C. A. Non steroid Antiinflammatory Agents. *Progress in Drug Research*. Birkhäuser Basel, 1966, 139-203.
50. Yang, Y., Zhang, Y. M., Chen, Y., Zhao, D., Chen, J. T., & Liu, Y., Construction of a graphene oxide based non covalent multiple nano supramolecular assembly as a scaffold for drug delivery, 2012, *Chemistry-A European Journal*, 18(14), 4208-4215.
51. Kumar V, Cotran R.S. Robbins S.L., (2003). Robbins Basic Pathology. 7th edition, WB Saunders Co, UK, ISBN:141602530, 2003:436-438
52. Lodish H, Berk A, Zipursky SL, Freeman.W.H (2000). Molecular Cell Biology. 4th edition New York.
53. Zhu, Y., Murali, S., Cai, W., Li, X., Suk, J. W., Potts, J. R., & Ruoff, R. S., Graphene and graphene oxide: synthesis, properties, and applications, *Advanced materials*, 2010, 22(35), 3906-3924.
54. Cioca, G. (1983). U.S. Patent No. 4,412,947. Washington, DC: U.S. Patent and Trademark Office.
55. Chvapil, M., Collagen sponge: theory and practice of medical applications, *Journal of biomedical materials research*, 1977, 11(5), 721-741.

56. Cockbill, S. M. E. (1998). Evaluation *In Vivo* And *In Vitro* Of The Performance Of Interactive Dressings In The Management Of Animal Soft Tissue Injuries, *Veterinary Dermatology*, 1998, 9, 87-98.
57. Eaglstein, W. H., Mertz, P. M., Marshall, D. A. Occlusive Wound Dressings to Prevent Bacterial Invasion and Wound Infection, *Journal of the American Academy of dermatology*, 1985, 12(4), 662-668.
58. Maser, Franz. (1996). Collagen Fibers, Foils And Hyaluronic Acid, Amide, Glucosamine And Galactosamine And Shrinkage. U.S. Patent No. 5,520,925.
59. Wicke, C., Halliday, B., Allen, D., Roche, N. S., Scheuenstuhl, H., Spencer, M. M., Hunt, T. K., Effects of steroids and retinoids on wound healing, *Archives of Surgery*, 2000, 135(11), 1265-1270.
60. Miyata, T. (1981). U.S. Patent No. 4,294,241. Washington, DC: U.S. Patent and Trademark Office.
61. Park, S., Ruoff, R. S., Chemical Methods For The Production Of Graphenes, *Nature Nanotechnology*, 2009, 4(4), 217-224.
62. Sheng, K., Sun, Y., Li, C., Yuan, W., Shi G, Ultrahigh-Rate Super capacitors Based On Electrochemically Reduced Graphene Oxide For Ac Line-Filtering, *Scientific reports*, 2012, 2, doi:10.1038/srep00247.
63. Stevens, M. M., Qanadilo, H. F., Langer, R., & Shastri, V. P., A Rapid-Curing Alginate Gel System: Utility In Periosteum-Derived Cartilage Tissue Engineering, *Biomaterials*, 2004, 25(5), 887-894.
